Plasma Metabolites Associated with OCT Features of Age-Related Macular Degeneration

Ines Lains, MD, PhD,[1] Xikun Han, PhD,[2,3] João Gil, MD,[4,5,6] Joana Providencia, MD,[4,5,6]
Archana Nigalye, MD,[1] Rodrigo Alvarez, MD,[1] Vivian Paraskevi Douglas, MD,[1] Kevin Mendez, MSc,[7]
Raviv Katz, BSc,[1] Gregory Tsougranis, BSc,[1] Jinglun Li, BSc,[8] Rachel S. Kelly, PhD,[7] Ivana K. Kim, MD,[1]
Jessica Lasky-Su, ScD,[7] Rufino Silva, MD, PhD,[4,5,6,9] Joan W. Miller, MD,[1] Liming Liang, PhD,[8]
Demetrios Vavvas, MD, PhD,[1] John B. Miller, MD,[1] Deeba Husain, MD[1]

Purpose: The most widely used classifications of age-related macular degeneration (AMD) and its severity stages still rely on color fundus photographs (CFPs). However, AMD has a wide phenotypic variability that remains poorly understood and is better characterized by OCT. We and others have shown that patients with AMD have a distinct plasma metabolomic profile compared with controls. However, all studies to date have been performed solely based on CFP classifications. This study aimed to assess if plasma metabolomic profiles are associated with OCT features commonly seen in AMD.

Design: Prospectively designed, cross-sectional study.

Participants: Subjects with a diagnosis of AMD and a control group (> 50 years old) from Boston, United States, and Coimbra, Portugal.

Methods: All participants were imaged with CFP, used for AMD staging (Age-Related Eye Disease Study 2 classification scheme), and with spectral domain OCT (Spectralis, Heidelberg). OCT images were graded by 2 independent graders for the presence of characteristic AMD features, according to a predefined protocol. Fasting blood samples were collected for metabolomic profiling (using nontargeted high-resolution mass spectrometry by Metabolon Inc). Analyses were conducted using logistic regression models including the worst eye of each patient (AREDS2 classification) and adjusting for confounding factors. Each cohort (United States and Portugal) was analyzed separately and then results were combined by meta-analyses. False discovery rate (FDR) was used to account for multiple comparisons.

Main Outcome Measures: Plasma metabolite levels associated with OCT features.

Results: We included data on 468 patients, 374 with AMD and 94 controls, and on 725 named endogenous metabolites. Meta-analysis identified significant associations (FDR < 0.05) between plasma metabolites and 3 OCT features: hyperreflective foci (6), atrophy (6), and ellipsoid zone disruption (3). Most associations were seen with amino acids, and all but 1 metabolite presented specific associations with the OCT features assessed.

Conclusions: To our knowledge, we show for the first time that plasma metabolites have associations with specific OCT features seen in AMD. Our results support that the wide spectrum of presentations of AMD likely include different pathophysiologic mechanisms by identifying specific pathways associated with each OCT feature.

Financial Disclosure(s): Proprietary or commercial disclosure may be found after the references. *Ophthalmology Science* 2024;4:100357 © 2023 by the American Academy of Ophthalmology. This is an open access article under the CC BY-NC-ND license (http://creativecommons.org/licenses/by-nc-nd/4.0/).

Supplemental material available at www.ophthalmologyscience.org.

Age-related macular degeneration (AMD) is a leading cause of blindness in people over the age of 50 years worldwide, and it is expected to affect 288 million people by 2040.[1] Conventional AMD classification schemes are based on color fundus photographs (CFPs) and categorize the early and intermediate forms of the disease based on the number and size of drusen and retinal epithelial pigment (RPE) changes. The advanced forms of AMD are classically categorized as wet or dry AMD depending on the presence of geographic atrophy or choroidal neovascularization, respectively. Despite the widespread use of this classification both in clinical practice and for research, it is currently well recognized that AMD has a wider phenotypic variability and that OCT offers important advantages in the assessment of AMD features.[2] For example, according to conventional classification

schemes,[3] an eye with a single classic drusen of more than 125 microns of size is classified as having intermediate AMD, whereas a patient with large confluent classic drusen, as well as multiple areas of subretinal drusenoid deposits (SDDs) and ellipsoid zone disruption, is also considered to have the same stage of disease. OCT has enabled clinicians to recognize that these 2 examples represent very distinct severities of disease[4] and has identified features of AMD that were previously not well recognized and are now known to have important prognostic value.[5,6] Thus, OCT is currently performed on a routine basis, and clinicians heavily rely on this technology both to diagnose and follow patients with AMD.

This spectrum of AMD phenotypes, especially as recognized by OCT, suggests that it is likely that AMD has multiple subtypes with different natural histories and prognoses. However, their pathophysiology remains largely unknown. This lack of knowledge has important consequences for clinical care because, for the majority of patients with the nonexudative forms of AMD, there are currently no available treatments.[7] A better understanding of the spectrum of AMD phenotypic presentations can point to novel pathogenic mechanisms and provide insights into possible targets for treatment.

Our Harvard Retinal Metabolomics group[8,9] and others[10] have shown that plasma metabolomics, the qualitative and quantitative analysis of metabolites ($<1-1.5$ kDa), can contribute to addressing these challenges and increase our current understanding of AMD pathophysiology.[11] Metabolites are the downstream product of the cumulative effects of the genome and its interaction with environmental exposures. Thus, the metabolome is thought to closely relate to disease phenotype, especially in multifactorial diseases like AMD.[12] To our knowledge, however, all AMD metabolomic studies performed to date based their assessment of this disease solely on CFPs, which, as mentioned, offer a limited perspective of the disease.

This study aimed to analyze associations between plasma metabolomic profiles and the presence of several OCT features commonly seen in AMD, with the ultimate goal of contributing to a better understanding of the wide spectrum of AMD phenotypes.

Methods

This work is part of a prospectively designed, cross-sectional study that was developed at 2 study sites: Boston, United States and Coimbra, Portugal. In Boston, patients were recruited at the Department of Ophthalmology of Massachusetts Eye and Ear (MEE) at Harvard Medical School (from the Retina Service and the Comprehensive Ophthalmology and Optometry Services). In Coimbra, Portugal, the study took place at the Faculty of Medicine of the University of Coimbra (FMUC), in collaboration with the Association for Innovation and Biomedical Research on Light and Image (AIBILI) and the "Centro Hospitalar e Universitário de Coimbra." All subjects enrolled in the study provided written informed consent.

The study protocol was conducted in accordance with the Health Insurance Portability and Accountability Act requirements and the tenets of the Declaration of Helsinki and was approved by the Institutional Review Boards of MEE/Massachusetts General Brigham, FMUC, and AIBILI and by the Portuguese National Data Protection Committee.

Eligibility Criteria

We included patients with a diagnosis of AMD as well as control subjects with no evidence of AMD and an age ≥ 50 years. At MEE, participants were consecutively recruited at their regular appointments. The Portuguese (FMUC/AIBILI) study population was derived from a population-based cohort study[13] in which all subjects with an established diagnosis of AMD were invited to participate. Subjects without signs of AMD in a prior evaluation[13] were also invited and included as controls if they remained without the disease in the present evaluation (see criteria below). For both cohorts, exclusion criteria included active uveitis or ocular infection, a diagnosis of any other vitreoretinal disease or diabetes, significant media opacities that precluded the observation of the ocular fundus, a refractive error ≥ 6 diopters of spheric equivalent, and any past history of retinal surgery as well as history of ocular surgery or intraocular procedure (such as laser and intraocular injections) within the 90 days before enrollment.

Of note, the study population considered for this work has been previously included in other manuscripts published by our group.[9]

Study Protocol

As previously described in detail,[8,14] at both study sites, all included participants underwent a bilateral dilated ophthalmic examination and were imaged with (1) CFPs, either with a Topcon TRC-50DX (Topcon Corporation) or a Zeiss FF-450Plus (Carl Zeiss Meditec) camera; and with (2) spectral domain-OCT (Spectralis). The initial spectral domain-OCT imaging protocol was an enhanced-depth imaging high-resolution volume centered in the fovea, with 61 lines, 30 × 25 degrees, and 30 frames Automatic Real Time. Due to the burden on patients, this was modified during the course of the study to an enhanced-depth imaging high-resolution volume with 97 lines, 20 × 20 degrees, and 15 frames Automatic Real Time.[15]

At the same visit, we also obtained a complete medical history according to a standardized questionnaire specifically built for the purposes of this study.[16] This included self-reported data on smoking habits (smokers were considered those who reported current smoking and ex-smokers those who have ever smoked, regardless of when they stopped), and weight and height (weight divided by the square of height was used to calculate body mass index [BMI] in the unit of kg/m^2). If the study participants did not know their current height and/or weight, these were recorded by a study investigator. All data was stored using REDCap electronic data capture tools.

Sample Collection and Mass Spectrometry Analysis

Blood samples were collected in the morning, after confirmed overnight fasting, into sodium-heparin tubes. As mentioned, in Boston, United States, patients were recruited at their regular appointments, so, for those not fasting at that time, a new appointment was scheduled for blood collection within a maximum of 1 month.

After collection, blood samples were centrifuged within 30 min (1500 rpm, 10 min, and 20°C), after which aliquots of 1.5 mL (MEE) and 5 mL (FMUC/AIBILI) were transferred into sterile cryovials and stored at −80°C. When all subjects had been recruited, plasma samples from Coimbra, Portugal, were shipped to

Table 1. Demographics and OCT Features of the Included Population

	Total	Boston, United States	Coimbra, Portugal
	n = 468	n = 183	n = 285
Age, yrs, mean ± SD	73.09 ± 7.96	71.73 ± 7.83	73.95 ± 7.94
Female sex, n (%)	300 (64.1)	117 (63.93)	183 (64.21)
BMI, kg/m^2, mean ± SD	27.20 ± 4.50	27.12 ± 4.66	27.26 ± 4.41
Ever smoker, n (%)	147 (31.41)	100 (54.64)	47 (16.49)
AREDS intake, n (%)	91 (19.44)	80 (43.72)	11 (3.86)
AMD status (AREDS classification)			
Control, n (%)	94 (20.09)	43 (23.5)	51 (17.89)
Early AMD, n (%)	86 (18.38)	30 (16.39)	56 (19.65)
Intermediate AMD, n (%)	192 (41.03)	64 (34.97)	128 (44.91)
Late AMD, n (%)	96 (20.51)	46 (25.14)	50 (17.54)
Classic drusen, n (%)	307 (65.74)	131 (71.58)	176 (61.97)
SDDs, n (%)	250 (53.42)	81 (44.26)	169 (59.3)
Atrophy, n (%)	96 (20.51)	51 (27.87)	45 (15.79)
EZ disruption, n (%)	214 (45.73)	99 (54.1)	115 (40.35)
Hyperreflective foci, n (%)	161 (34.62)	65 (35.52)	96 (34.04)
Drusenoid PED, n (%)	25 (13.66)	25 (13.66)	NA
Serous PED, n (%)	25 (5.98)	7 (5.26)	18 (6.32)
Evidence of exudative AMD, n (%)	103 (22.01)	36 (19.67)	67 (23.51)

AMD = age-related macular degeneration; AREDS = Age-Related Eye Disease Study; BMI = body mass index; EZ = ellipsoid zone; NA = not available for the Portuguese population; PED = pigment epithelial detachment; SDD = subretinal drusenoid deposit.

MEE in dry ice (through TNT Express). Then, all samples (i.e., from both study locations) were shipped to Metabolon Inc, also in dry ice (through TNT Express). In both cases, samples arrived frozen in < 48 hours and were immediately stored at −80°C until processing.

AMD Diagnosis and Staging

As the patients included in this work had already been considered for previous manuscripts published by our group,[9] CFPs were already graded for AMD and AMD stage. Briefly, field 2 CPF images were initially standardized.[17] Images taken with Topcon cameras were evaluated with IMAGEnet 2000 software (version 2.56; Topcon Medical Systems), and those obtained with a Zeiss camera were observed using VISUPAC (version 4.5.1; Carl Zeiss Meditec). After standardization, AMD diagnosis and staging was performed by 2 independent experienced graders according to the Age-Related Eye Disease Study (AREDS) classification system[3,18]: controls: presence of drusen maximum size < circle C0 and total area < C1; early AMD: drusen maximum size ≥ C0 but < C1 or presence of AMD characteristic pigment abnormalities in the inner or central subfields; intermediate AMD: presence of drusen maximum size ≥ C1 or of drusen maximum size ≥ C0 if the total area occupied is > I2 for soft indistinct drusen and > O2 for soft distinct drusen; late AMD: presence of geographic atrophy (or "dry" late AMD) or evidence of choroidal neovascularization AMD (or "wet" AMD). In case of disagreement, a senior author (R.S. or D.H.) established the final categorization.

OCT Grading

For this work, 2 independent investigators, masked to the remaining data, analyzed all the OCT volume scans for the presence or absence (dichotomous variable) of the following features: ellipsoid zone disruption; classic drusen (defined as sub-RPE deposits; presence of ≥ 1 drusen was graded as "yes"); SDDs[19]

(presence of ≥ 1 was graded as "yes"); hyperreflective foci (HRF) (presence of ≥ 1 was graded as "yes"); retinal atrophy (defined as presence of at least incomplete RPE and outer retinal atrophy[20]); serous pigment epithelium detachment; and evidence of current or past exudative AMD (defined as presence of subretinal fluid, intraretinal fluid, or fibrosis). In the Boston cohort the presence of drusenoid pigment epithelium detachments was also assessed (requiring at least more than one-half disc diameter in size). A senior author (R.S. or D.H.) resolved any cases of disagreement.

Metabolomic Profiling and Data Processing

Plasma samples were shipped to Metabolon Inc in dry ice, arrived frozen in < 24 hours, and were immediately stored at −80°C until processing. Nontargeted mass spectrometry analysis was performed using ultrahigh performance liquid chromatography-tandem mass spectrometry, according to previously published protocols.[8] For this work, samples were merged from 2 stages of metabolomic profiling: samples from a pilot study (n=120 from Boston)[8] and the remaining samples.[9] Considering this, a batch normalization method, in which the raw metabolite measurements were divided by the median values in each instrument batch, was used to combine all metabolic data. We subsequently performed our quality control and data processing pipeline[11,21] using metabolomicsR package (version 1.0.0). Briefly, metabolites with missing rate > 50%, unnamed metabolites, and exogenous metabolites were excluded from the subsequent analysis. We detected measurement outliers defined as values > 5 standard deviations, and those were winsorized. Missing values were imputed with half of the minimum value in each batch.[22] Then, metabolite measurements were log-transformed and standardized to interpret the effect sizes of metabolites in the unit of per standard deviation change. This led to a total of 725 named endogenous metabolites that were then used for analyses.

Table 2. Multivariable Analysis of Metabolites Associated with Summary Score of OCT Features

Metabolite	Super Pathway	Sub Pathway	HMDB	β Boston	P value Boston	β Coimbra	P value Coimbra	β meta	FDR meta
N-Acetylasparagine	Amino acid	Alanine and aspartate metabolism	HMDB0006028	0.565	0.000	0.362	0.001	0.432	0.0006
N-Acetylleucine	Amino acid	Leucine, isoleucine, and valine metabolism	HMDB0011756	0.468	0.003	0.361	0.002	0.399	0.0039
Histidine	Amino acid	Histidine metabolism	HMDB0000177	−0.721	1.5×10^{-6}	−0.145	0.183	−0.352	0.0072
β-citrylglutamate	Amino acid	Glutamate metabolism	NA	0.507	0.001	0.275	0.013	0.353	0.0085
Hypotaurine	Amino acid	Methionine, cysteine, SAM, and taurine metabolism	HMDB0000965	0.079	0.636	0.446	8.8×10^{-5}	0.332	0.0222
1-Carboxyethylleucine	Amino acid	Leucine, isoleucine and valine metabolism	NA	0.227	0.175	0.397	0.001	0.341	0.0222
N-Acetylisoleucine	Amino acid	Leucine, isoleucine and valine metabolism	HMDB0061684	0.440	0.006	0.229	0.045	0.301	0.0375
N-Acetylphenylalanine	Amino acid	Phenylalanine metabolism	HMDB0000512	0.278	0.084	0.322	0.006	0.307	0.0375
N-Acetylglutamine	Amino acid	Glutamate metabolism	HMDB0006029	0.565	3.3×10^{-4}	0.153	0.171	0.294	0.0375
1-Carboxyethylphenylalanine	Amino acid	Phenylalanine metabolism	NA	0.175	0.269	0.345	0.002	0.288	0.0443
Taurine	Amino acid	Methionine, cysteine, SAM, and taurine metabolism	HMDB0000251	0.261	0.088	0.277	0.009	0.272	0.0485
N-Acetylglucosamine/N-acetylgalactosamine	Carbohydrate	Aminosugar metabolism	HMDB0000212, HMDB0000215	0.577	4.1×10^{-4}	0.244	0.033	0.357	0.0116
Maltose	Carbohydrate	Glycogen metabolism	HMDB0000163	0.125	0.422	0.385	3.3×10^{-4}	0.302	0.0266
Maltotriose	Carbohydrate	Glycogen metabolism	HMDB0001262	0.094	0.554	0.377	0.001	0.286	0.0408
α-Tocopherol	Cofactors and vitamins	Tocopherol metabolism	HMDB0001893	0.806	8.4×10^{-8}	0.127	0.251	0.378	0.0039
α-CMBHC glucuronide	Cofactors and vitamins	Tocopherol metabolism	NA	0.685	4.0×10^{-8}	0.245	0.056	0.413	0.0067
Carotene diol (2)	Cofactors and vitamins	Vitamin A metabolism	NA	0.573	2.5×10^{-4}	0.244	0.023	0.352	0.0072
Carotene diol (3)	Cofactors and vitamins	Vitamin A metabolism	NA	0.629	5.4×10^{-5}	0.156	0.214	0.347	0.0222
Ascorbic acid 3-sulfate*	Cofactors and vitamins	Ascorbate and aldarate metabolism	NA	0.506	0.002	0.234	0.033	0.320	0.0222
Carotene diol (1)	Cofactors and vitamins	Vitamin A metabolism	NA	0.527	0.001	0.183	0.087	0.295	0.0309
Malate	Energy	TCA cycle	HMDB0031518,HMDB0000156,HMDB0000744	0.286	0.066	0.307	0.006	0.300	0.0333
Octadecenedioylcarnitine (C18:1-DC)*	Lipid	Fatty acid metabolism (acyl carnitine, dicarboxylate)	NA	−0.447	0.004	−0.248	0.023	−0.315	0.0222
2-Hydroxyglutarate	Lipid	Fatty acid, dicarboxylate	HMDB0059655	0.410	0.008	0.264	0.018	0.314	0.0240
Linoleoyl-docosahexaenoyl-glycerol (18:2/22:6) [2]*	Lipid	Diacylglycerol	HMDB0007266	−0.374	0.023	−0.274	0.012	−0.305	0.0309
Octadecanedioylcarnitine (C18-DC)*	Lipid	Fatty acid metabolism (acyl carnitine, dicarboxylate)	NA	−0.352	0.025	−0.250	0.020	−0.283	0.0408
Cytidine	Nucleotide	Pyrimidine metabolism, cytidine containing	HMDB0000089	0.564	2.4×10^{-4}	0.149	0.177	0.293	0.0369

FDR = false discovery rate; HMDB = Human Metabolome Database identifier; meta = results from meta-analysis; NA = not available; SAM = S-adenosylmethionine; TCA = tricarboxylic acid.

Table 3. Results of Multivariable Analysis for Metabolites Associated with Hyperreflective Foci

Metabolite	Super Pathway	Sub Pathway	HMDB	β Boston	P value Boston	β Coimbra	P value Coimbra	β meta	FDR meta
N-Acetylasparagine	Amino acid	Alanine and aspartate metabolism	HMDB0006028	0.51	0.005	0.38	0.017	0.43	0.0387
β-Citrylglutamate	Amino acid	Glutamate metabolism	NA	0.94	1.6×10^{-5}	0.55	4.9×10^{-4}	0.68	0.0001
Hypotaurine	Amino acid	Methionine, cysteine, SAM, and taurine metabolism	HMDB0000965	0.16	0.400	0.83	2.8×10^{-6}	0.52	0.0218
Taurine	Amino acid	Methionine, cysteine, SAM, and taurine metabolism	HMDB0000251	0.34	0.049	0.49	0.001	0.43	0.0340
Phosphoethanolamine	Lipid	Phospholipid metabolism	HMDB0000224	0.21	0.238	0.62	1.6×10^{-4}	0.43	0.0419
Hypoxanthine	Nucleotide	Purine metabolism, (hypo)xanthine/ inosine containing	HMDB0000157	0.14	0.434	0.77	3.7×10^{-6}	0.47	0.0218

FDR = false discovery rate; HMDB = Human Metabolome Database identifier; NA = not available; meta = results from meta-analysis, SAM = S-adenosylmethionine.

Statistical Analysis

Descriptive statistics were used to summarize the demographic and clinical characteristics of the study population, including mean and standard deviation for continuous variables and percentages for categorical variables.

First, we computed a sum score of the different OCT features assessed (ranging between 0 features to 8 features present), and multivariable linear regression models were used to evaluate associations between metabolites and the OCT features' sum score. The goal of this first analysis was to serve as a starting point to assess and explore if there were associations between having an increasing number of OCT features and changes in metabolite levels, given that this strategy enables more statistical power than assessing each OCT feature alone.

However, because we were particularly interested in the relationships of each specific OCT feature and plasma metabolite, we then proceeded to calculate them using multivariable logistic regression models (the outcome for each OCT feature was coded as 0 if not present and 1 if present), adjusting for age, sex, BMI, and smoking. To evaluate the predictive ability of the identified metabolites, receiving operating characteristic (ROC) curves were built for: a baseline model (model A) that included age, sex, BMI, and smoking status and a model B that included the metabolites identified as significantly associated with each OCT features in addition to the variables of the baseline model. The pROC package (version 1.18.0)

was used to visualize and compare ROC curves. A sensitivity analysis was also performed adjusting for AREDS intake as a covariate.

All tests were initially conducted separately in each study site (Boston, United States, and Coimbra, Portugal), and then fixed-effect meta-analyses were performed. To account for the multiple testing, we used false discovery rate (FDR, Benjamini and Hochberg method).[23] False discovery rate corrected P values < 0.05 were defined as significant and are presented.

Results

We included 468 individuals, 183 (39%) from Boston, United States, and the remaining (n = 285, 61%) from Coimbra, Portugal. Among them, 94 (20%) were classified as controls (mean age, 67.9 ± 6.6 years), and the remaining were classified as having AMD (mean age for early AMD 70.1 ± 6.2, intermediate AMD 74.3 ± 7.4, and late AMD 78.3 ± 7.7). Table 1 presents the demographics of the included study population as well as the prevalence of the different OCT features assessed. As expected, although some of the OCT features were highly correlated among them, others were not (Fig S1A, B, available at www.ophthalmologyscience.org).
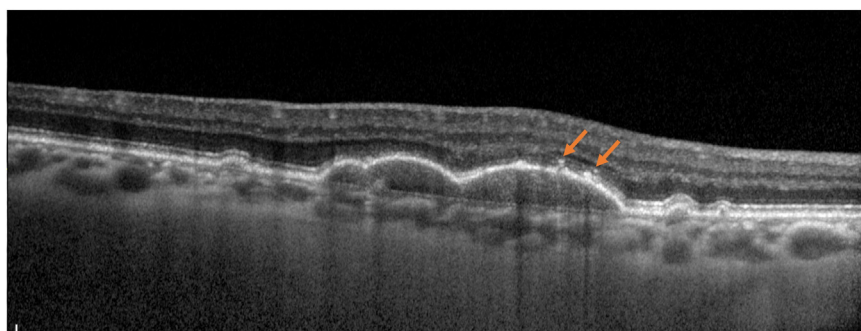

Figure 2. Representative OCT b-scan demonstrating hyperreflective foci (orange arrows) overlying a large drusenoid pigment epithelial detachment.
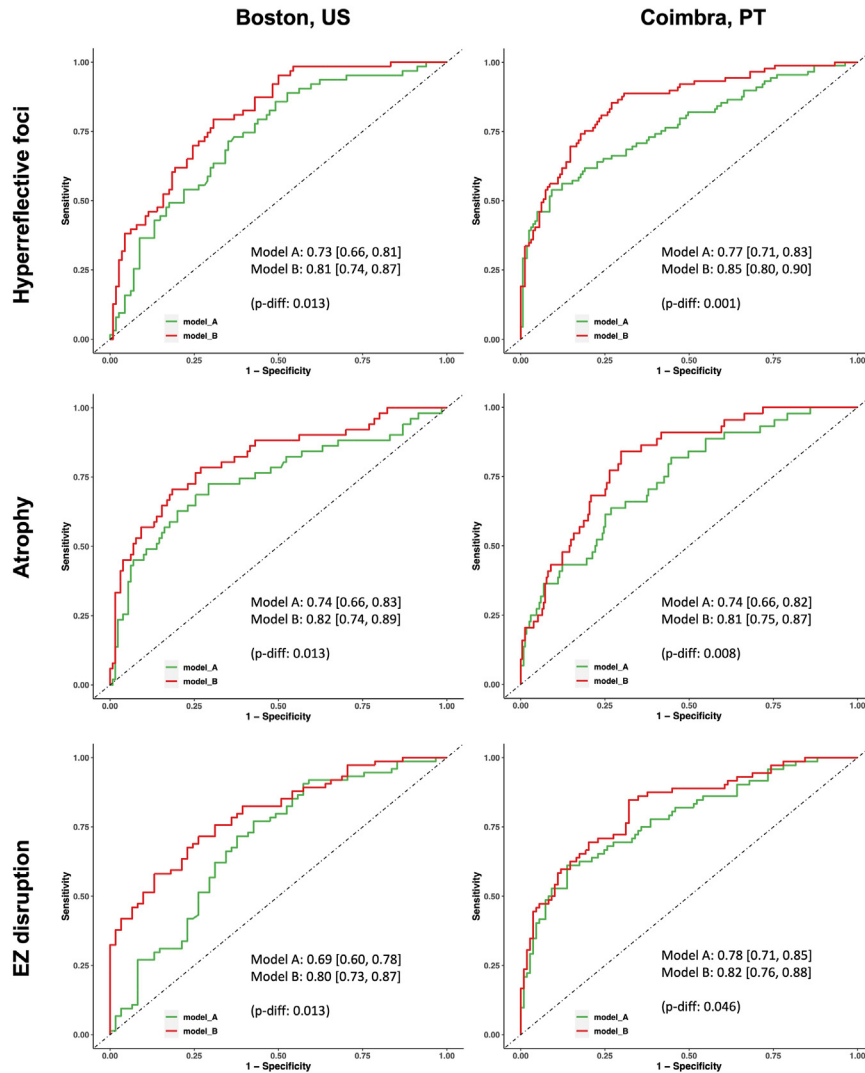
Figure 3. Receiving operating characteristic curves for OCT features with significant associations with metabolites. In these figures, model A includes age, sex, body mass index, and smoking status. Model B includes metabolites identified as significantly associated with each OCT feature in addition to the variables of the baseline model (i.e., for hyperreflective foci, metabolites listed in Table 3; for atrophy, metabolites listed in Table 4; and for ellipsoid zone disruption, metabolites listed in Table 5).

Sum Score

As explained in the Methods section, we started by developing a summary score incorporating the different OCT features assessed (ranging between 0 features to 8 features present). Our results revealed that 32 metabolites had statistically significant associations with this score (Table 2). Most associations were seen with amino acids (n = 14; 43.8%). In particular, N-acetylasparagine showed the most significant association (*P* value FDR = 0.0006), with results revealing that, per standard deviation change of in the levels of this metabolite, the sum score increased by 0.43.

Metabolites Associated with HRF

We then assessed associations between metabolites and each OCT feature independently. Accounting for confounding factors, meta-analysis identified 6 metabolites significantly associated with HRF (FDR *P* value < 0.042). Most (n = 4) were amino acids, with 2 belonging to the taurine metabolism pathway. Table 3 details these results. Figure 2 presents an example of an OCT b-scan with HRF.

Compared with a baseline model of only age, sex, BMI, and smoking status, the addition of the identified significant metabolites improved the ability to discriminate the presence of HRF both in Boston, United States, and Coimbra, Portugal (Fig 3; *P* = 0.013 and 0.001, respectively).

Metabolites Associated with Atrophy

After accounting for FDR, meta-analysis also identified 6 metabolites associated with the presence of atrophy (Fig 4). All of them were different than those associated with HRF and are listed in Table 4. Adding the identified 6
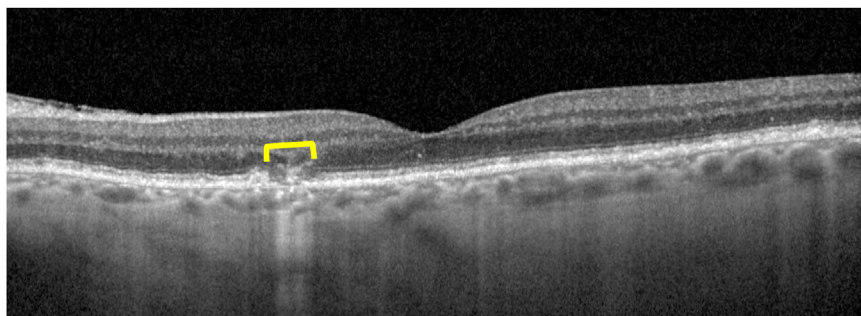
Figure 4. OCT b-scan demonstrating presence of atrophy (yellow arrow) — in this case incomplete retinal pigment epithelium and outer retinal atrophy (iRORA).

metabolites to a model with clinical covariates alone also significantly improved the ability to discriminate for the presence of atrophy (Fig 3; $P < 0.013$).

Metabolites Associated with Ellipsoid Zone Disruption

Meta-analyses also identified 3 metabolites associated with the presence of ellipsoid disruption on OCT (Fig 5). These metabolites are listed in Table 5. Figure 3 shows the ROC curves of the ability to discriminate for the presence of ellipsoid disruption with and without considering the identified metabolites.

Associations with OCT Features Not Meeting FDR Criteria

For the remaining OCT features assessed (i.e., classic drusen, SDDs, serous pigment epithelium detachment, and fluid), no plasma metabolites showed significant associations after accounting for multiple comparisons. However, when considering a P value of < 0.01 (unadjusted P value), there were 8 plasma metabolites associated with the presence of classic drusen (Table S6, available at www.ophthalmologyscience.org), 10 with associations with SDDs (Table S7, available at www.

ophthalmologyscience.org), and 25 with the presence of fluid (Table S8, available at www.ophthalmologyscience.org).

Analysis Additionally Accounting for AREDS Intake

As an important percentage of the included patients was taking AREDS vitamins, we performed an additional analysis accounting for AREDS vitamin intake. As shown in Table 9, when additionally accounting for this variable, 3 significant associations were seen with HRF, and 3 others were seen with the presence of atrophy. All these associations were among the statistical associations seen without adjusting for this covariate (i.e., also shown in Tables 3 and 4).

Discussion

We present a cross-sectional study assessing associations between plasma metabolites and specific OCT features commonly seen in patients with AMD in 2 cohorts, one from Boston, United States, and the other from Coimbra, Portugal. The results of our meta-analysis accounting for multiple comparisons identified plasma metabolites

Table 4. Results of Multivariable Analysis for Metabolites Associated with Atrophy

Metabolite	Super Pathway	Sub Pathway	HMDB	β Boston	P value Boston	β Coimbra	P value Coimbra	β meta	FDR meta
N-Acetylglutamate	Amino acid	Glutamate metabolism	HMDB0001138	0.417	0.028	0.627	0.002	0.516	0.0358
N-Acetylleucine	Amino acid	Leucine, isoleucine, and valine metabolism	HMDB0011756	0.675	0.001	0.464	0.016	0.560	0.0283
N-Acetylphenylalanine	Amino acid	Phenylalanine metabolism	HMDB0000512	0.480	0.015	0.501	0.007	0.491	0.0367
N-Acetyltyrosine	Amino acid	Tyrosine metabolism	HMDB0000866	0.601	0.003	0.394	0.031	0.488	0.0367
N-Acetylglucosamine/ N-acetylgalactosamine	Carbohydrate	Aminosugar metabolism	HMDB0000212, HMDB0000215	0.792	1.7×10^{-4}	0.489	0.013	0.630	0.0086
Malate	Energy	TCA cycle	HMDB0031518, HMDB0000156 HMDB0000744	0.445	0.015	0.512	0.004	0.479	0.0358

FDR = false discovery rate; HMDB = Human Metabolome Database identifier; meta = results from meta-analysis; TCA = tricarboxylic acid.
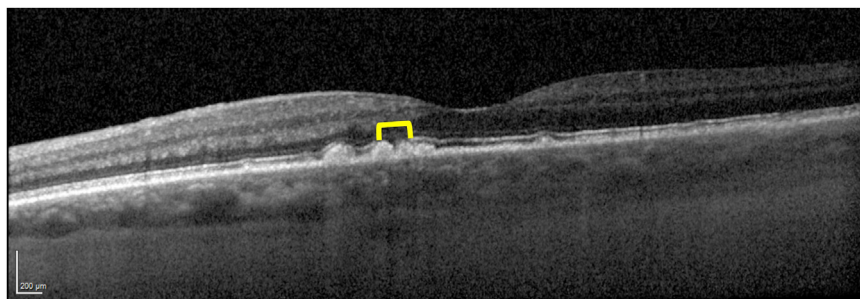
Figure 5. OCT b-scan demonstrating presence of ellipsoid disruption (yellow brackets) in an area overlying classic drusen.

associated with 3 OCT features. In particular, the highest number and the most significant associations were seen with the presence of HRF and atrophy (n = 6 for both, most of them amino acids). Additionally, a sum score incorporating the 8 OCT features evaluated revealed that levels of 32 metabolites were associated with a higher likelihood of having an increasing number of findings on OCT.

To our knowledge, this is the first time that metabolomic−OCT associations have been performed in the context of AMD as well as in ophthalmology in general. Color fundus photographs are a good representation of fundus examinations, but their limitations in the assessment of AMD and other retinal diseases are now well recognized. OCT is currently the preferred modality to evaluate and follow patients with AMD, and it has provided important insights into the wide spectrum of presentations of this disease, especially its dry nonadvanced forms. In our study, specific groups of metabolites were associated with 3 OCT features that are known to have prognostic value in patients with AMD: HRF, outer retinal atrophy, and ellipsoid zone disruption. Importantly, there was almost no overlap among the metabolites related with each one of these OCT parameters, which supports the hypothesis that AMD may comprise different pathogenic mechanisms. This is relevant because it points to potential new pathways that in the future can be further explored as possible treatment targets.

In particular, in this work we identified strong associations between plasma metabolites and HRF, which are discrete lesions with equivalent or higher reflectivity than the RPE band on OCT.[24] Histologically, HRF are thought to represent the migration of RPE cells toward the retinal surface.[25] They are also considered to reflect, at least partially, the health of the RPE[24] and have been proposed as a potentially useful structural end point for studies on preventing progression of intermediate to advanced AMD.[26]

Interestingly, all the metabolites in this work that showed an association with HRF have also been described by our group as differing among patients with AMD and controls when solely assessing the disease based on CFPs.[9] Among them are taurine, the most abundant amino acid in the retina, and hypotaurine, its precursor.[27,28] The exact local function of taurine and hypotaurine remains unknown, but they have been recognized to have an antioxidant and neuroprotective role.[29,30] Studies suggest that taurine depletion increases oxidative stress and impairs the phagocytic capacity of the RPE,[31] thus leading to degeneration of photoreceptors and RPE.[28,32] On the other hand, it has been shown that taurine administration can promote RPE cell proliferation.[33] The positive association seen in this work between hypotaurine and taurine, and the presence of HRF raises the possibility that this may represent a compensatory response to RPE degeneration.

The presence of HRF was also associated with phosphoethanolamine, a direct precursor of phosphatidylethanolamine, which is a dominant glycerophospholipid in the retina.[34] Importantly, both our group[8,9] and others[35,36] have consistently shown dysregulations of the glycerophospholipid pathway in patients with AMD. The observed association with HRF might be related to the fact that in the outer segments of the photoreceptors, phosphatidylethanolamines participate in the formation of A2E, which is the most important component of

Table 5. Results of Multivariable Analysis for Metabolites Associated with Ellipsoid Zone Disruption

Metabolite	Super pathway	Sub pathway	HMDB	β Boston	P value Boston	β Coimbra	P value Coimbra	β meta	FDR meta
N-Acetylasparagine	Amino acid	Alanine and aspartate metabolism	HMDB0006028	0.800	2.2×10^{-5}	0.415	0.005	0.562	0.0011
α-CMBHC glucuronide	Cofactors and vitamins	Tocopherol metabolism	NA	0.810	8.2×10^{-5}	0.299	0.066	0.496	0.0368
Linoleoyl-docosahexaenoyl-glycerol (18:2/22:6)	Lipid	Diacylglycerol	HMDB0007266	−0.497	0.007	−0.403	0.009	−0.442	0.0435

FDR = false discovery rate; HMDB = Human Metabolome Database identifier; meta = results from meta-analysis; NA = not available.

Table 9. Results of Multivariable Analysis for Plasma Metabolites with Significant Associations with OCT Features When Additionally Accounting for AREDS Intake

	Metabolite	Super pathway	Sub pathway	HMDB	β Boston	P value Boston	β Coimbra	P value Coimbra	β meta	FDR meta
Atrophy	N-acetylglutamate	Amino acid	Glutamate metabolism	HMDB0001138	0.494	0.019	0.604	0.003	0.551	0.037
	N-Acetylglucosamine/ N-Acetylgalactosamine	Carbohydrate	Aminosugar metabolism	HMDB0000212, HMDB0000215	0.746	0.001	0.472	0.017	0.594	0.037
	Malate	Energy	Tricarboxylic acid cycle	HMDB0031518, HMDB0000156, HMDB0000744	0.510	0.009	0.503	0.005	0.507	0.037
Hyperreflective foci	β-Citrylglutamate	Amino acid	Glutamate metabolism	NA	0.851	2.3×10^{-4}	0.556	0.001	0.655	1.2×10^{-4}
	Hypotaurine	Amino acid	Methionine, cysteine, SAM, and taurine metabolism	HMDB0000965	0.186	0.368	0.806	0.000	0.542	0.015
	Hypoxanthine	Nucleotide	Purine metabolism, (hypo) xanthine/inosine containing	HMDB0000157	0.175	0.362	0.764	0.000	0.508	0.015

FDR = false discovery rate; HMDB = Human Metabolome Database identifier; meta = results from meta-analysis; NA = not available; SAM = S-adenosylmethionine; TCA = tricarboxylic acid.

lipofuscin[37] and is toxic to the RPE.[38] Indeed, a recent study described that hyperreflective specks (i.e., hyperreflective dots similar to HRF but of smaller size) are composed of lipofuscin granules.[6]

Two amino acids, which are part of the alanine, aspartate, and glutamate metabolism pathway, were also shown in this work to relate to HRF. Briefly, alanine and aspartate are nonessential amino acids that generate glutamate, which has a role as a neurotransmitter,[39,40] and participate in mitochondrial energy metabolism. However, elevated levels of glutamate can be pathogenic, leading to photoreceptor cell death[41] and RPE cell proliferation.[42] Indeed, dysregulations in the glutamate pathway have been proposed as an important mechanism of proliferative vitreoretinopathy, which seems to share pathogenic mechanisms with the formation of HRF.[43] It is also remarkable to note that metabolites in the alanine, aspartate, and glutamate pathway have consistently been reported as being dysregulated in AMD.[41] Besides the work by our group,[9,14,44] a recent study by the Eye-Risk Consortium showed that glutamine and glutaminolysis were among the most predictive features to discriminate between patients with nonadvanced AMD and controls.[35]

In this work, we also identified important associations with the presence of outer retinal atrophy, one of them a metabolite that also belongs to the glutamate pathway: N-acetylglutamate. This is not surprising considering that, as mentioned above, dysregulations in this pathway have been linked to photoreceptor cell death.[41] Three other amino acids also showed an association with atrophy (N-acetylphenylalanine, N-acetylleucine, and N-acetyltyrosine). Understanding the mechanisms of these associations is more challenging, but consistent work has reported dysregulations of several amino acids in AMD,[8–10] in particular, of N-acetylleucine, the acetylated form of leucine, which seems to be primarily used for protein synthesis in the retina.[45] This is essential, considering the daily shed of the photoreceptors' outer segments. Additionally, in animal models, leucine (and other branch chain amino acids) has been shown to suppress photoreceptor cell death,[46] even when administered at late stages of retinal degeneration.[46] In our initial work, increased levels of N-acetylleucine were associated with more advanced stages of AMD.[9] In this work, a positive association was also seen with atrophy, which suggests that this may represent a compensatory response to halt RPE cell death and further progression of atrophy. Dysregulations of phenylalanine have also been reported in AMD both by our group and others.[10] Phenylalanine is an essential amino acid that, by hydroxylation, can led to the formation of tyrosine, which is then a precursor of both dopamine and melanin.[47] With aging, melanin in the RPE undergoes oxidative modifications, which decrease its antioxidant capacity[48,49] and thus can contribute to retinal degeneration.[47] Indeed, oxidative stress has been shown to be a crucial pathogenic mechanism of AMD.

This work is not without limitations. First, this is a cross-sectional study, and its design does not allow for the establishment of causality. In particular, it is unclear if the

reported changes in plasma metabolites are driving the development of the OCT features that they are associated with or if, conversely, they are a consequence of these structural changes. Secondly, in this work, we included patients with AMD and controls, but a sensitivity analysis accounting for AMD stages and AMD status showed comparable effect sizes to the estimates reported here. Additionally, all metabolomic assessments were performed in the plasma, and retinal tissue evaluations are required to understand if the described dysregulations are also seen in situ. We also did not account for the possible effect of environmental factors (such as dietary patterns) in the reported results, and these may at least partially explain some of the differences observed between our 2 cohorts. Additionally, in this work, OCT features were characterized as binary outcomes (i.e., yes/no) and not quantified, which could provide additional important information. Finally, even though all samples used in this study were collected after confirmed overnight fasting and we focused on endogenous metabolites, nutritional parameters and medications are known to affect metabolomic profiles, and we did not include them in our analyses. Of note, however, we performed a subanalysis accounting for intake of AREDS vitamins (in addition to the remaining covariates), and the metabolites with the most significant associations with HRF and atrophy maintained their significance, which further supports the relevance of these associations but also highlights that some associations might be related to exogenous factors not accounted for.

In conclusion, to our knowledge, we present the first report that plasma metabolites have specific associations with OCT features commonly seen in AMD. In particular, the highest number and the most significant associations were seen with HRF and atrophy. Taken together, these results contribute to a better understanding of the pathophysiology of the wide spectrum of presentations of dry AMD by identifying specific pathways associated with each OCT feature. Further studies are needed to characterize the identified pathways and help elucidate AMD subtypes. We believe that this work paves the way for the identification of potential druggable targets for AMD, ultimately helping reduce the burden of blindness in this disease.

Footnotes and Disclosures

[1] Department of Ophthalmology, Massachusetts Eye and Ear, Harvard Medical School, Boston, Massachusetts.

[2] Department of Epidemiology, Harvard T H Chan School of Public Health, Boston, Massachusetts.

[3] Program in Genetic Epidemiology and Statistical Genetics, Harvard T H Chan School of Public Health, Boston, Massachusetts.

[4] Faculty of Medicine, University of Coimbra, Coimbra, Portugal.

[5] Ophthalmology Department, Centro Hospitalar e Universitário de Coimbra, Coimbra, Portugal.

[6] Association for Innovation and Biomedical Research on Light and Image, Coimbra, Portugal.

[7] Systems Genetics and Genomics Unit, Channing Division of Network Medicine Brigham and Women's Hospital and Harvard Medical School, Boston, Massachusetts.

[8] Department of Biostatistics, Harvard T H Chan School of Public Health, Boston, Massachusetts.

[9] Clinical Academic Center of Coimbra (CCAC), Coimbra, Portugal.

References

1. Wong WL, Su X, Li X, et al. Global prevalence of age-related macular degeneration and disease burden projection for 2020 and 2040: a systematic review and meta-analysis. *Lancet Glob Health*. 2014;2:e106−e116.

2. de Sisternes L, Simon N, Tibshirani R, et al. Quantitative SD-OCT imaging biomarkers as indicators of age-related macular degeneration progression. *Invest Ophthalmol Vis Sci*. 2014;55: 7093−7103.

3. Danis RP, Domalpally A, Chew EY, et al. Methods and reproducibility of grading optimized digital color fundus photographs in the Age-Related Eye Disease Study 2 (AREDS2 Report Number 2). *Invest Ophthalmol Vis Sci*. 2013;54:4548−4554.

4. Leuschen JN, Schuman SG, Winter KP, et al. Spectral-domain optical coherence tomography characteristics of intermediate age-related macular degeneration. *Ophthalmology*. 2013;120: 140−150.

5. Waldstein SM, Vogl WD, Bogunovic H, et al. Characterization of Drusen and hyperreflective foci as biomarkers for disease progression in age-related macular degeneration using artificial intelligence in optical coherence tomography. *JAMA Ophthalmol*. 2020;138:740−747.

6. Echols BS, Clark ME, Swain TA, et al. Hyperreflective foci and specks are associated with delayed rod-mediated dark adaptation in nonneovascular age-related macular degeneration. *Ophthalmol Retina*. 2020;4:1059−1068.

7. Ung C, Lains I, Miller JW, Kim IK. Current management of age-related macular degeneration. In: Crusio WE, Dong H, Radeke HH, et al., eds. *Advances in Experimental Medicine and Biology*. New York, NY: Springer; 2021:295−314.

8. Laíns I, Kelly RS, Miller JB, et al. Human plasma metabolomics study across all stages of age-related macular degeneration identifies potential lipid biomarkers. *Ophthalmology*. 2018;125:245−254.

9. Laíns I, Chung W, Kelly RS, et al. Human plasma metabolomics in age-related macular degeneration: meta-analysis of two cohorts. *Metabolites*. 2019;9:127.

10. Acar İE, Lores-Motta L, Colijn JM, et al. Integrating metabolomics, genomics, and disease pathways in age-related macular degeneration: the EYE-RISK Consortium. *Ophthalmology*. 2020;127:1693−1709.

11. Laíns I, Gantner M, Murinello S, et al. Metabolomics in the study of retinal health and disease. *Prog Retin Eye Res*. 2019;69:57−79.

12. Nicholson JK, Holmes E, Kinross JM, et al. Metabolic phenotyping in clinical and surgical environments. *Nature*. 2012;491:384−392.

13. Cachulo M da L, Lobo C, Figueira J, et al. Prevalence of age-related macular degeneration in Portugal: the Coimbra Eye Study - report 1. *Ophthalmologica*. 2015;233:119−127.

14. Laíns I, Duarte D, Barros AS, et al. Human plasma metabolomics in age-related macular degeneration (AMD) using nuclear magnetic resonance spectroscopy. *PLOS ONE*. 2017;12:e0177749.

15. Laíns I, Miller JB, Park DH, et al. Structural changes associated with delayed dark adaptation in age-related macular degeneration. *Ophthalmology*. 2017;124:1340−1352.

16. Laíns I, Miller JB, Mukai R, et al. Health conditions linked to age-related macular degeneration associated with dark adaptation. *Retina*. 2018;38:1145−1155.

17. Tsikata E, Laíns I, Gil J, et al. Automated brightness and contrast adjustment of color fundus photographs for the grading of age-related macular degeneration. *Transl Vis Sci Technol*. 2017;6:3.

18. Age-Related Eye Disease Study Research Group. The Age-Related Eye Disease Study system for classifying age-related macular degeneration from stereoscopic color fundus photographs: the Age-Related Eye Disease Study report number 6. *Am J Ophthalmol*. 2001;132:668−681.

19. Spaide RF, Curcio CA. Anatomical correlates to the bands seen in the outer retina by optical coherence tomography: literature review and model. *Retina*. 2011;31:1609−1619.

20. Guymer RH, Rosenfeld PJ, Curcio CA, et al. Incomplete retinal pigment epithelial and outer retinal atrophy in age-

related macular degeneration: classification of atrophy meeting report 4. *Ophthalmology*. 2020;127:394−409.

21. Han X, Liang L. metabolomicsR: a streamlined workflow to analyze metabolomic data in R. *Bioinform Adv*. 2022;2: vbac067.

22. Dekkers KF, Sayols-Baixeras S, Baldanzi G, et al. An online atlas of human plasma metabolite signatures of gut microbiome composition. *Nat Commun*. 2022;13:5370.

23. Benjamini Y, Hochberg Y. Controlling the false discovery rate: a practical and powerful approach to multiple testing. *J R Stat Soc*. 1995;57:289−300.

24. Christenbury JG, Folgar FA, O'Connell RV, et al. Progression of intermediate age-related macular degeneration with proliferation and inner retinal migration of hyperreflective foci. *Ophthalmology*. 2013;120:1038−1045.

25. Tiosano L, Byon I, Alagorie AR, et al. Choriocapillaris flow deficit associated with intraretinal hyperreflective foci in intermediate age-related macular degeneration. *Graefes Arch Clin Exp Ophthalmol*. 2020;258:2353−2362.

26. Curi R, Lagranha CJ, Doi SQ, et al. Molecular mechanisms of glutamine action. *J Cell Physiol*. 2005;204:392−401.

27. Ripps H, Shen W. Review: taurine: a "very essential" amino acid. *Mol Vis*. 2012;18:2673−2686.

28. Hadj-Saïd W, Froger N, Ivkovic I, et al. Quantitative and topographical analysis of the losses of cone photoreceptors and retinal ganglion cells under taurine depletion. *Invest Ophthalmol Vis Sci*. 2016;57:4692−4703.

29. Tomi M, Terayama T, Isobe T, et al. Function and regulation of taurine transport at the inner blood−retinal barrier. *Microvasc Res*. 2007;73:100−106.

30. Ando D, Kubo Y, Akanuma S, et al. Function and regulation of taurine transport in Müller cells under osmotic stress. *Neurochem Int*. 2012;60:597−604.

31. Pasantes-Morales H, Cruz C. Taurine and hypotaurine inhibit light-induced lipid peroxidation and protect rod outer segment structure. *Brain Res*. 1985;330:154−157.

32. Gaucher D, Arnault E, Husson Z, et al. Taurine deficiency damages retinal neurones: cone photoreceptors and retinal ganglion cells. *Amino Acids*. 2012;43:1979−1993.

33. Shin EY, Park JH, Shin ME, et al. Injectable taurine-loaded alginate hydrogels for retinal pigment epithelium (RPE) regeneration. *Mater Sci Eng C Mater Biol Appl*. 2019;103:109787.

34. Fliesler SJ. Lipids and lipid metabolism in the eye. *J Lipid Res*. 2010;51:1−3.

35. Kersten E, Dammeier S, Ajana S, et al. Metabolomics in serum of patients with non-advanced age-related macular degeneration reveals aberrations in the glutamine pathway. *PLOS ONE*. 2019;14:e0218457.

36. Zhang M, Jiang N, Chu Y, et al. Dysregulated metabolic pathways in age-related macular degeneration. *Sci Rep*. 2020;10:2464.

37. Kim HJ, Montenegro D, Zhao J, Sparrow JR. Bisretinoids of the retina: photo-oxidation, iron-catalyzed oxidation, and disease consequences. *Antioxidants (Basel)*. 2021; 10:1382.

38. Wolf G. Lipofuscin and macular degeneration. *Nutr Rev*. 2003;61:342−346.

39. Ishikawa M. Abnormalities in glutamate metabolism and excitotoxicity in the retinal diseases. *Scientifica (Cairo)*. 2013;2013:528940.

40. Boldyrev A, Bulygina E, Makhro A. Glutamate receptors modulate oxidative stress in neuronal cells. A mini-review. *Neurotox Res*. 2004;6:581−587.

41. Han G, Wei P, He M, Teng H. Glucose metabolic characterization of human aqueous humor in relation to wet age-related macular degeneration. *Invest Ophthalmol Vis Sci*. 2020; 61:49.

42. García S, López E, López-Colomé AM. Glutamate accelerates RPE cell proliferation through ERK1/2 activation via distinct receptor-specific mechanisms. *J Cell Biochem*. 2008;104: 377−390.

43. Curcio CA, Zanzottera EC, Ach T, et al. Activated retinal pigment epithelium, an optical coherence tomography biomarker for progression in age-related macular degeneration. *Invest Ophthalmol Vis Sci*. 2017;58(6): BIO211−BIO226.

44. Lains I, Mendez K, Nigalye A, et al. Plasma metabolomic profiles associated with three-year progression of age-related macular degeneration. *Metabolites*. 2022;12:32.

45. Xu R, Ritz BK, Wang Y, et al. The retina and retinal pigment epithelium differ in nitrogen metabolism and are metabolically connected. *J Biol Chem*. 2020;295:2324−2335.

46. Hasegawa T, Ikeda HO, Iwai S, et al. Branched chain amino acids attenuate major pathologies in mouse models of retinal degeneration and glaucoma. *Heliyon*. 2018;4: e00544.

47. Zeng L, Li X, Liu J, et al. RNA-seq analysis reveals an essential role of the tyrosine metabolic pathway and inflammation in myopia-induced retinal degeneration in guinea pigs. *Int J Mol Sci*. 2021;22:12598.

48. Hou XW, Wang Y, Pan CW. Metabolomics in age-related macular degeneration: a systematic review. *Invest Ophthalmol Vis Sci*. 2020;61:13.

49. Żądto A, Ito S, Sarna M, et al. The role of hydrogen peroxide and singlet oxygen in the photodegradation of melanin. *Photochem Photobiol Sci*. 2020;19:654−667.